The *ham-2* Locus, Encoding a Putative Transmembrane Protein, Is Required for Hyphal Fusion in *Neurospora crassa*

Qijun Xiang, Carolyn Rasmussen and N. Louise Glass[1]

Plant and Microbial Biology Department, University of California, Berkeley, California 94720-3102

Manuscript received August 15, 2001
Accepted for publication October 30, 2001

ABSTRACT

Somatic cell fusion is common during organogenesis in multicellular eukaryotes, although the molecular mechanism of cell fusion is poorly understood. In filamentous fungi, somatic cell fusion occurs during vegetative growth. Filamentous fungi grow as multinucleate hyphal tubes that undergo frequent hyphal fusion (anastomosis) during colony expansion, resulting in the formation of a hyphal network. The molecular mechanism of the hyphal fusion process and the role of networked hyphae in the growth and development of these organisms are unexplored questions. We use the filamentous fungus *Neurospora crassa* as a model to study the molecular mechanism of hyphal fusion. In this study, we identified a deletion mutant that was restricted in its ability to undergo both self-hyphal fusion and fusion with a different individual to form a heterokaryon. This deletion mutant displayed pleiotropic defects, including shortened aerial hyphae, altered conidiation pattern, female sterility, slow growth rate, lack of hyphal fusion, and suppression of vegetative incompatibility. Complementation with a single open reading frame (ORF) within the deletion region in this mutant restored near wild-type growth rates, female fertility, aerial hyphae formation, and hyphal fusion, but not vegetative incompatibility and wild-type conidiation pattern. This ORF, which we named *ham-2* (for *h*yphal *a*nasto*m*osis), encodes a putative transmembrane protein that is highly conserved, but of unknown function among eukaryotes.

FILAMENTOUS fungi grow by tip extension, branching, and hyphal fusion (anastomosis) to form a hyphal network that makes up a fungal individual (Buller 1933; Xiang and Morris 1999). Although tip growth and branching have been extensively studied in filamentous fungi (Riquelme *et al.* 1998), essentially nothing is known about the mechanism or function of hyphal fusion in the growth and development of filamentous fungi. Hyphal fusion is presumably a way to increase cytoplasmic flow and interconnectedness of hypha. Further, intrahyphal communication may influence hyphal pattern formation and developmental processes (Rayner 1996).

Hyphal anastomosis in filamentous fungi has been described in the literature (Buller 1933). The initiation of hyphal anastomosis most likely involves the production of a diffusible signal(s) (Gooday 1975) that mediates positive autotropism and polarized hyphal tip growth (Buller 1933; McCabe *et al.* 1999). Once participating hyphae physically contact each other, a breakdown of the cell wall ensues, followed by fusion of the plasma membrane and cytoplasmic mixing. Major alterations in cytoplasmic flow between hyphae can be observed upon completion of the fusion process (P. Hickey, D. Jacobson, N. Read and L. Glass, unpublished observations).

Hyphal fusion takes place not only between hyphae within a fungal colony; it can also occur between hyphae from different colonies. In the latter case, hyphal anastomosis results in the formation of a heterokaryon in which genetically different nuclei coexist in a common cytoplasm (Glass *et al.* 2000; Saupe 2000). Formation of viable heterokaryons can be restricted by *het*erokaryon incompatibility (*het*) loci. The presence of alternative alleles at a *het* locus in a common cytoplasm (by the formation of partial diploids, heterokaryon formation, or transformation) results in growth inhibition, suppression of conidiation, and hyphal compartmentation and death.

Hyphal fusion in filamentous fungi is comparable to cell fusion events in other organisms. Examples include fertilization events between egg and sperm and somatic cell fusion events that result in a syncytium, such as myoblast fusion during muscle differentiation (Taylor 2000). Although somatic cell fusion events have been studied intensively in more complex eukaryotes, the molecular mechanism of cell and membrane fusion is still poorly understood. Our goal is to understand the molecular mechanism of formation of the hyphal network. Identification and characterization of mutants that fail to undergo hyphal fusion may reveal the function of a process that is ubiquitous and probably universal in this group of organisms. Understanding the mo-

[1]*Corresponding author:* Department of Plant and Microbial Biology, 111 Koshland Hall, University of California, Berkeley, CA 94720-3102. E-mail: lglass@uclink.berkeley.edu

lecular mechanism of the hyphal fusion process in filamentous fungi may provide a paradigm for somatic cell fusion events in other eukaryotic organisms.

In this study, we isolated a deletion mutant in the filamentous fungus *Neurospora crassa* that had a reduced capacity to undergo both self- and non-self-hyphal fusion during vegetative growth. This mutant displayed a slow growth rate, female sterility, shortened aerial hyphae, altered conidiation pattern, and also suppressed *het-c*-mediated vegetative incompatibility. We determined that a single open reading frame (ORF) within the deletion region in the mutant was required for hyphal fusion and wild-type aerial hypha formation, but not vegetative incompatibility or wild-type conidiation patterns. We named this locus *ham-2*, for *h*yphal *a*nastomosis, because of the similarity in phenotype between mutants that contain mutations in this ORF and another hyphal fusion mutant, *ham-1* (Wilson and Dempsey 1999). The *ham-2* gene product is predicted to encode a plasma membrane protein that is highly conserved, but of unknown function, in other eukaryotic organisms.

MATERIALS AND METHODS

***N. crassa* strains and growth media:** The strains used in this study are listed in Table 1. Strains were maintained on Vogel's medium (Vogel 1964) with required supplements. Crosses were performed on 1× Westergaard's medium (Westergaard and Mitchell 1947) with one-tenth to one-twentieth of the concentration of supplements normally provided in vegetative growth medium, as required. Complementation of female fertility defects in mutants can be obtained by forming a heterokaryon between protoperithecial defective strains (such as *ham-2*) and Fungal Genetics Stock Center (FGSC) 4564. The strain FGSC 4564 (Table 1) has a mutation in the mating-type locus and cannot participate in a cross, but forms female reproductive structures (protoperithecia; Griffiths and Delange 1978; Perkins 1984; Staben and Yanofsky 1990). Such heterokaryons were used as females in crosses. Mating type of progeny was determined by crosses with mating-type testers *fl A* (FGSC 4317) and *fl a* (FGSC 4347; Table 1).

Heterokaryon tests: Strains with auxotrophic markers were cultured in Vogel's medium (Vogel 1964) with supplements. To assess the capacity of mutant strains to undergo hyphal fusion, we used three assays. In the first assay, 1 μl each from conidial suspensions (~10^7 conidia/ml in water) from two strains containing complementing auxotrophic markers were co-inoculated onto Vogel's medium either in a petri dish or in a race tube. Growth of the heterokaryons was recorded every 24 hr. A second, modified heterokaryon test was developed to assess whether mutants retained any capacity to undergo hyphal fusion. In this case, conidial suspensions from two auxotrophic strains were inoculated onto a plate in two separate spots, 1 cm apart. The plates contained limited amounts of required nutrients: 8 μm uridine for *pyr-4* mutants, 1.5 μm adenine for *ad-3A* or *ad-3B* mutants, 3 μm L-arginine for *arg-5* mutants, and 7 μm L-threonine for *thr-2* mutants. Conidial germination and growth occurred, but growth was sparse. In the region of mycelial contact between the two strains, a successful heterokaryon was visualized by rapid growth from the contact area, caused by complementation of auxotrophic markers after hyphal fusion. If a heterokaryon was not formed, the growth of the strains eventually stopped due to nutritional limitation. In the third assay, we determined hyphal fusion frequency. A conidial suspension of a heterokaryon tester strain (a strain with auxotrophic markers) of known amount of viable conidia (10^5 conidia/plate) was mixed with varying amounts of a conidial suspension from a hyphal fusion mutant or wild type (with complementing auxotrophic markers; 10^2, 10^3, 10^4, and 10^5 conidia). Conidial suspensions were plated onto media that cause *N. crassa* to grow as compact colonies (BdeS; Davis and De Serres 1970). After 3 days of growth, the number of colonies on each plate was recorded.

Nucleic acid isolation and Southern hybridization: Genomic DNA was isolated from mycelia ground in liquid nitrogen or dried mycelia as described in Lee and Taylor (1990). A [^{32}P-dCTP]-labeled probe was generated using the T7 QuickPrime kit (Amersham Pharmacia Biotech) and Southern hybridization was performed as described in Sambrook *et al.* (1989). Probes used in this study were *Xba*I6.5, *Bam*HI9-4 (Figures 3 and 4), and *Apa*I-*Not*I (AN3-2; Figure 3). Probes were made from restriction fragments from cosmid H57:G1.

Cloning strategy: A linkage group (LG) V-specific genomic cosmid library constructed in vector pLorist6xh (conferring hygromycin resistance) was obtained from Fungal Genetics Stock Center (Department of Microbiology, University of Kansas Medical Center, http://www.kumc.edu/research/fgsc/). DNA was isolated from the library by using a Midiprep kit (QIAGEN, Valencia, CA). Transformation was performed as described in Schweizer *et al.* (1981). Introduced DNA (via transformation protocols) usually integrates randomly at ectopic positions in the genome of *N. crassa*. Various pools of cosmid DNA from the LGV library were introduced into *N. crassa* until a single cosmid that complemented the aerial hyphae defect in strain 8-88 (Table 1) was identified by sib selection (Akins and Lambowitz 1985). The DNA sequence at one end of the *N. crassa* insert in H57:G1 was determined using a primer to the SP6 site within the pLoristxh vector. DNA sequence determinations were performed using the ABI automated DNA sequencing procedure at the DNA Sequencing Facility (Berkeley, CA; http://idrive.berkeley.edu/dnaseq/web). Contig searches were performed by using the BLAST programs provided at the Munich Information Center for Protein Sequences (MIPS; http://www.mips.biochem.mpg.de/proj/neurospora/). Subcloning was performed using DNA sequence, predicted ORFs, and restriction sites in contig 9a36 (http://www.mips.biochem.mpg.de/proj/neurospora/) and cosmid H57:G1. DNA fragments from H57:G1 (Figures 3 and 4) were cloned into a plasmid conferring hygromycin resistance, pCB1004 (Carroll *et al.* 1994), for transformation into *N. crassa*.

Computational analyses: Transmembrane prediction programs used were TOP-PRED (http://bioweb.pasteur.fr/seqanal/interfaces/toppred.html), TMAP (http://130.237.130.31/tmap/single.html), and Split 35 (http://pref.etfosa.hr.split/). These three programs correctly predicted the number of transmembrane regions in a benchmark protein, a Ca^{2+} ATPase from rabbit; the number of transmembrane domains in this Ca^{2+} ATPase has been experimentally determined (Toyoshima *et al.* 2000). Signal peptide predictions for putative proteins used SignalP (http://www.cbs.dtu.dk/service/SignalP). BLAST database searches were conducted at the National Center for Biotechnology Information (NCBI) site (http://www.ncbi.nlm.nih.gov/BLAST/).

Light microscopy: Sterile pieces of cellophane (Fisher Scientific, Pittsburgh) were spread onto the surface of solid medium and inoculated with conidia. After 24 hr, the pieces of cellophane bearing the mycelia were peeled off from the surface of the medium and placed onto slides. The hyphae were examined under bright field or differential interference contrast

using either an Olympus BH-2 or a Zeiss Axioskop II microscope. Samples were also prepared by inoculating conidia directly onto solid media (without cellophane) and culturing for 24 or 48 hr. Photographs of perithecial contents and hyphae were taken by a Hamamatsu digital CCD camera (Hamamatsu, Japan) and images were analyzed using Open*lab* from Improvision (Coventry, United Kingdom). Photographs of perithecial contents (×100 and ×400) were taken after staining with lactophenol cotton blue.

RESULTS

Identification of a pleiotropic mutant: We identified a mutant that displayed multiple phenotypic defects during a screen for suppressors of *het-c*-mediated vegetative incompatibility in *N. crassa*. Transformants containing *het-c* alleles of alternative specificity display inhibited growth, lack aerial hyphae and conidia, and show hyphal compartmentation and death (Saupe *et al.* 1996; Saupe and Glass 1997; Wu and Glass 2001). We introduced a plasmid that confers hygromycin resistance and that contained a *het-c*^{OR} allele (Saupe *et al.* 1996) into a strain of alternative *het-c* specificity (C9-2 *het-c*^{PA}; Table 1). Transformation methods most often result in ectopic integration of introduced DNA in *N. crassa* and thus most of these transformants were heterozygous for *het-c* (*het-c*^{OR} and *het-c*^{PA}). We picked 90 hygromycin-resistant transformants that displayed *het-c* vegetative incompatibility to agar slants (referred to as "incompatible" transformants). Sixty of these incompatible transformants escaped from *het-c*-mediated vegetative incompatibility, which was associated with an abrupt increase in conidiation. Escape from vegetative incompatibility in heterokaryons and partial diploids that were heterozygous for a *het* locus has previously been correlated with deletions of one of the duplicated *het* loci or mutations at unlinked suppressor loci (Newmeyer 1970; Delange and Griffiths 1975; Vellani *et al.* 1994; Smith *et al.* 1996). These previously described escape events were also associated with an abrupt increase in growth rate and conidiation.

One of the escape transformants, b-11-1 (Table 1), displayed short aerial hyphae and copious conidiation. b-11-1 was crossed with the wild-type strain RLM 57-30 (*pyr-4 het-c*^{OR} *A*; Table 1) and 106 progeny were examined from the cross. Sixty-two progeny had a wild-type phenotype, while 44 progeny showed shortened aerial hyphae and copious conidiation, a ratio compatible with 1:1 by a χ^2 test. The mutant progeny also showed a slower growth rate than wild-type isolates, ~3 cm/day, as compared to the 6- to 7-cm/day growth rate of a wild-type strain and occasionally produced orange-colored bodies throughout the colony. We refer to this segregating mutation as *ahc*, for *a*erial *h*yphae and *c*onidiation (Figure 1).

To determine whether *het-c* specificity cosegregated with the aerial hyphae and conidiation defects in the *ahc* progeny, we performed heterokaryon tests with conidial suspensions from the *ahc* phenotypic class of progeny and wild-type *het-c* tester strains (OR-type, I-1-83 and I-1-51; PA-type, Xa-2 and Xa-3; Table 1). Of the 32 tested *ahc* progeny, 14 were classified as *het-c*^{OR} and 18 typed as *het-c*^{PA}, indicating that the *ahc* mutation was unlinked to the *het-c* locus. Four of the *ahc het-c*^{PA} progeny were hygromycin resistant, indicating that the ectopic copy of *het-c*^{OR} (and pCB1004) was linked to the *het-c* locus in the original b-11-1 transformant. We did not identify any *het-c* null strains from the 32 *ahc* progeny characterized from this cross. In *N. crassa,* duplicated sequences (such as the alternative *het-c* sequences in the C9-2 transformants) suffer GC to AT transition mutations in both resident and ectopic copies of these sequences when such strains are taken through a cross (Selker 1997). This mutagenic phenomenon has been termed repeat induced point (RIP) mutation; *het-c* null strains have been isolated previously by using this method (Saupe *et al.* 1996). Four *ahc* progeny showed partial *het-c*^{PA} function (fully compatible with a *het-c*^{PA} tester and partially incompatible with a *het-c*^{OR} tester; heterokaryons grew at a faster rate than typical *het-c* incompatible heterokaryons but showed a similar phenotype), suggesting that these strains may contain mutations in *het-c* that result in partial function of HET-C^{PA}. The partial loss of the *het-c* function class presumably resulted from mutations in *het-c*^{PA} induced by RIP mutation.

The (*ahc* + wild type) heterokaryons of identical *het-c* specificity displayed a near wild-type growth rate, normal conidiation, and aerial hyphae formation, indicating that the *ahc* mutation was recessive. However, heterokaryon formation between the *ahc* progeny and the wild-type *het-c* testers was delayed; heterokaryons between *ahc* strains and wild-type strains were observed after 2–3 days, rather than the normal time of 1 day or less for heterokaryons to form between two wild-type strains.

The *ahc* mutation suppresses *het-c* vegetative incompatibility: The *ahc* progeny displayed vegetative incompatibility in heterokaryons with wild-type strains that contained alleles that conferred alternative *het-c* specificity. To determine if the *ahc* mutation also suppressed *het-c* vegetative incompatibility in a recessive manner, we attempted to force heterokaryons between *ahc; pyr-4 het-c*^{OR} and *ahc; thr-2 het-c*^{PA} progeny (Table 1) using conidial suspensions. However, prototrophic heterokaryons were not observed after 5 days of incubation. To determine if the ability to form a heterokaryon was affected in *ahc* strains of identical *het-c* specificity, we crossed strain 8-88 (*het-c*^{OR} *pyr-4; ahc A*) with FGSC 4070 (*het-c*^{OR}*; lys-1 a*) and recovered *het-c*^{OR}*; lys-1; ahc* and *het-c*^{OR}*; pyr-4; ahc* progeny (Table 1). The *lys-1; ahc* progeny were tested for heterokaryon formation with *pyr-4; ahc* progeny using conidial suspensions. No visible heterokaryotic growth was observed after 5 days of incubation.

We developed a modified heterokaryon test whereby (*pyr-4 het-c*^{OR}*; ahc* + *thr-2 het-c*^{PA}*; ahc*) and (*pyr-4 het-c*^{OR};

TABLE 1

***N. crassa* strains**

Strain	Genotype[a]	Origin/cross
C9-2	*het-c^{PA} thr-2 a*	Smith *et al.* (1996)
RLM 57-26	*pyr-4 arg-5; inl; pan-2 a*	Gift from R. L. Metzenberg
RLM 57-30	*cyh-1; pyr-4 A*	Gift from R. L. Metzenberg
I-1-83	*ad-3A his-3 A*	Gift from A. J. F. Griffiths
I-1-51	*ad-3A nic-2 a*	Gift from A. J. F. Griffiths
C9-15	*het-c^{PA} thr-2 A*	Smith *et al.* (1996)
Xa-2	*het-c^{PA} arg-5; pan-2 a*	C9-15 × RLM 57-26
Xa-3	*het-c^{PA} arg-5; pan-2 A*	C9-15 × RLM 57-26
FGSC 997	*T(I-II) al-I; T(IV-V) cot-I; T(III-VI) ylo I A*	FGSC[b]
FGSC 1144	*ilv-2 a*	FGSC
FGSC 7168	*cyh-2 leu-5 a*	FGSC
FGSC 2164	*lys-2 a*	FGSC
FGSC 4070	*lys-1 a*	FGSC
FGSC 4317	*fl A*	FGSC
FGSC 4347	*fl a*	FGSC
FGSC 4564	*ad-3B cyh-1 a^{ml}*	FGSC
b-11-1	*het-c^{PA} thr-2; ahc (het-c^{OR}) a*	Escape transformant
8-88	*pyr-4; ahc A*	b-11-1 × RLM 57-30
8-56	*pyr-4; ahc a*	b-11-1 × RLM 57-30
39-8	*lys-1 ahc A*	8-88 × FGSC 4070
39-12	*lys-1 ahc a*	8-88 × FGSC 4070
8-16	*thr-2 het-c^{PA}; ahc A*	b-11-1 × RLM 57-30
8-17	*thr-2 het-c^{PA}; ahc a*	b-11-1 × RLM 57-30
9-1-5	*pyr-4 A*	b-19-5 (an escape transformant) × RLM57-30
Crl-10	*pyr-4; ham-2 A*	RIP progeny from C9-2 (AN3-2) × 9-1-5
Cr3-3	*pyr-4; ham-2; pan-2 A*	Cr1-10 × R5-47
Cr3-6	*ham-2; pan-2 A*	Cr1-10 × R5-47
Cr3-12	*ham-2 A*	Cr1-10 × R5-47
Cr3-17	*pyr-4; ham-2 a*	Cr1-10 × R5-47
Cr3-20	*pyr-4; ham-2 A*	Cr1-10 × R5-47
R5-47	*his-5 tol trp-4; pan-2 a*	Shiu and Glass (1999)
R1-08	*a* (ORS 8-1)	Gift of R. L. Metzenberg

[a] All strains are Oak Ridge compatible (including *het-c*) unless otherwise noted.
[b] FGSC, Fungal Genetics Stock Center (http://www.fgsc.net/).

ahc + *lys-1 het-c^{OR}; ahc*) heterokaryons could be recovered (see materials and methods). Conidial suspensions from two auxotrophic *ahc* strains were inoculated in two separate spots 1 cm apart onto a plate that contained limiting amounts of required nutrients. Successful heterokaryotic growth was visualized by rapid growth from the contact area between the two sparsely growing colonies, caused by complementation of auxotrophic markers after hyphal fusion. Heterokaryons between *ahc* strains that contained *het-c* alleles of alternative specificity (*pyr-4 het-c^{OR}; ahc* + *thr-2 het-c^{PA}; ahc*) were phenotypically similar to heterokaryons between *ahc* strains of identical *het-c* specificity (*pyr-4 het-c^{OR}; ahc* + *lys-1 het-c^{OR}; ahc*), indicating that the *ahc* mutation also suppressed *het-c* vegetative incompatibility.

The frequency of heterokaryon formation is reduced in the *ahc* mutant: We determined the frequency of heterokaryon formation between an *ahc* mutant and a wild-type strain as compared to heterokaryon formation between two wild-type strains (see materials and methods). Approximately 16 heterokaryotic colonies were observed when ~60 viable conidia from 9-1-5 (*pyr-4*; *A*) were mixed with 1.3×10^5 viable conidia from FGSC 4564 (*ad-3B cyh-1 a^{m1}*) and spread onto plates (Table 2). By contrast, the frequency of heterokaryon formation between an *ahc* mutant (8-88) and a wild-type strain (FGSC 4564) was reduced >1000-fold (to 6.2×10^{-4}; Table 2). We did not observe hyphal fusion bridges in colonies of the *ahc* mutant in extensive microscopic analyses, suggesting that the reduced capacity of 8-88 to form a heterokaryon is due to a defect in the hyphal fusion process.

The *ahc* mutant shows sexual defects: Strains containing the *ahc* mutation failed to make female reproductive structures (protoperithecia) and were thus female sterile. This defect was also recessive; female fertility in an *ahc* mutant could be restored by forcing a heterokaryon between 8-88 and FGSC 4564 (*ad-3B cyh-1 a^{m1}*, Table 1; see materials and methods). Heterozygous crosses between 8-88 × wild type produced

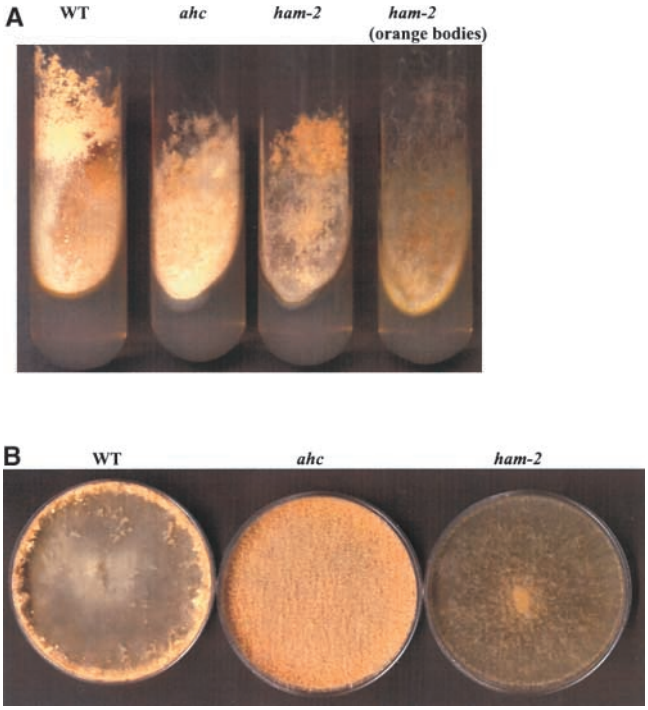

FIGURE 1.—(A) Strains of *N. crassa* grown in Vogel's (VOGEL 1964) medium in test tubes. Note the short aerial hyphae in the *ahc* and *ham-2* mutants as compared to a wild-type strain. The large orange bodies seen in the *ahc* and *ham-2* mutants are shown in the test tube on the far right (*ham-2* mutant is shown). (B) Strains of *N. crassa* grown on plates of vegetative medium for 1 week. Note the copious amount of conidia that cover the entire plate in the *ahc* mutant, as compared to a wild-type strain, which conidiates around the margin of the plate. The *ham-2* mutant is more similar to wild-type in its conidiation pattern than to the *ahc* mutant.

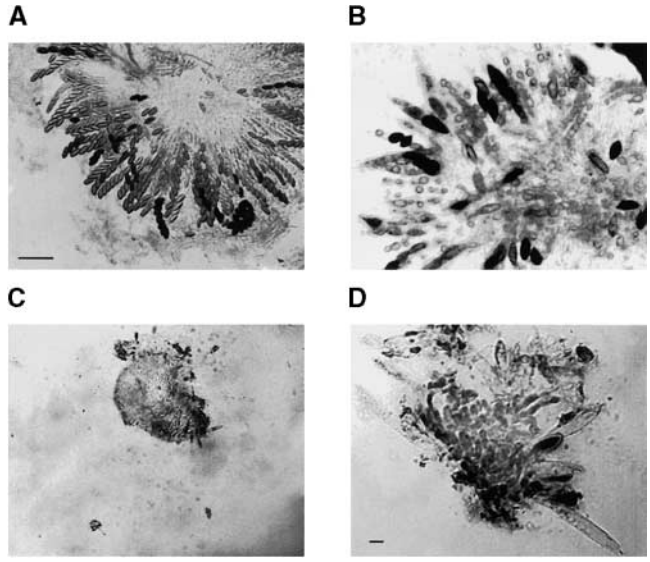

FIGURE 2.—Perithecial squashes from crosses of *N. crassa* strains. (A) Perithecial contents from a *ham-2* × wild-type cross (Cr3-12 × R1-08; Table 1) (bar, 100 μm). Note the numerous asci containing eight ascospores. Mature asci contain eight black ascospores. The phenotype of heterozygous crosses with *ham-2* are similar to wild-type crosses, although formation of the rosettes is delayed by ~1 week. (B) Perithecial squash from an *ahc* mutant (8-88; Table 1) crossed with wild type (I-1-51). In this cross, 8-88 was used as a male. Note the numerous asci that are devoid of ascospores. The few ascospores that are seen are variable in size and pigmentation (same magnification as in A). (C) Perithecial squash from a homozygous *ham-2* [(Cr3-3 + FGSC 4564) × Cr3-12; Table 1] cross (same magnification as in A). Note the absence of normal size and numbers of asci and complete lack of ascospore progeny. (D) Enlargement of perithecial contents from C (bar, 10 μm).

only 1% viable progeny (Figure 2B). The number of ascospores was greatly reduced in these crosses and only a small proportion of these ascospores germinated to give viable progeny. The ratio between *ahc* mutant and wild-type progeny in these crosses was near 1:1. The ascus dominant phenotype of the *ahc* mutant occurred whether the *ahc* mutant was used as a male or as a female (in a heterokaryon with FGSC 4564) in crosses with wild- type strains. Homozygous crosses between *ahc* mutants [(8-88 + FGSC 4564) × 8-17; Table 1] were completely sterile.

The *ahc* mutation maps to linkage group V: The mapping strain ALCOY (FGSC 997; Table 1) was used to map the *ahc* mutation in 8-88 by following the morphology of the shortened aerial hyphae in progeny of the crosses. The *ahc* mutation mapped to the right arm of linkage group V, closely linked to *lys-2*. Only 1 recombinant out of 151 progeny was recovered in a cross between 8-88

TABLE 2

Frequency of heterokaryon formation

Strain	Viable conidia	Reference strain	Viable conidia	No. of colonies	Frequency
9-1-5	60	FGSC 4564	1.3×10^5	16 ± 1	1
8-88	1.2×10^5	FGSC 4564	1.3×10^5	2 ± 1	6.2×10^{-4}
Cr1-10	1×10^5	FGSC 4564	1.3×10^5	0–1	2.5×10^{-4}
8-88 (Xhk5-4)	1×10^{5a}	FGSC 4564	1.3×10^5	41 ± 8	1.6×10^{-3}

[a] Due to the heterokaryotic nature of transformants in *N. crassa*, the conidial concentration of a 8-88 (Xhk5-4) transformant was determined by counting the number of conidia under the microscope via a hemacytometer rather than by assessing viable conidia by plate counts.

and FGSC 2164 (*lys-2*; Table 1). Out of 102 progeny, 1 recombinant was identified in a cross between 8-88 and FGSC 1144 (*ilv-2*). And out of a total of 182, 18 recombinant progeny were recovered in a cross between 8-88 and a *leu-5* strain (FGSC 7168). Since *lys-2* lies between *ilv-2* and *leu-5*, these data indicate that the *ahc* mutation maps between *lys-2* and *ilv-2* on linkage group V.

Cosmid H57:G1 complements the *ahc* mutant phenotype: Heterokaryon tests indicated that the aerial hyphae defect of the *ahc* mutant was recessive. Thus, we hypothesized that it would be possible to complement the aerial hyphae defect of 8-88 by DNA-mediated transformation with a cosmid library from *N. crassa*. Pools from a chromosome V-specific genomic library (obtained from the FGSC; see MATERIALS AND METHODS) were subdivided successively and introduced into 8-88 until a single cosmid that complemented the aerial hyphae defect was identified (H57:G1).

The introduction of the cosmid H57:G1 complemented the vegetative phenotypic defects of 8-88. The 8-88 transformants bearing H57:G1 displayed near wild-type growth rates (5–6 cm/day), normal aerial hyphal differentiation, and a normal conidiation pattern and lacked orange bodies. Heterokaryons between 8-88 transformants bearing H57:G1 and a wild-type strain (I-1-83; Table 1) were easily formed using conidial suspensions. Heterokaryons between 8-88 (H57:G1) transformants and an *ahc* strain of alternative *het-c* allelic specificity, 8-16 (*het-c*^{PA}; Table 1), displayed an incompatible phenotype, indicating that *het-c*-mediated vegetative incompatibility had been restored to 8-88 by the introduction of H57:G1.

Using an SP6 primer, the DNA sequence of the end of the *N. crassa* insert in H57:G1 was determined. These sequences were used to search the *N. crassa* linkage group II and V database (http://www.mips.biochem.mpg.de/proj/neurospora/). The H57:G1 cosmid was determined to be in the middle of contig 9a36 on LGV, as predicted by genetic analyses. Subsequent restriction site mapping of H57:G1 and comparison to the predicted restriction sites indicated that the cosmid lay between nucleotide position ~47303 and 86174 in contig 9a36, ~39 kbp. Thirteen ORFs were predicted to be in this region (Figure 3).

A subclone of H57:G1 containing a single ORF complemented the aerial hyphae, growth rate, and hyphal fusion defects of the *ahc* mutant, but not conidiation pattern defects or vegetative incompatibility: Deletion analysis of cosmid H57:G1 indicated that the cosmid lost its ability to complement the aerial hyphae defect when introduced into strain 8-88 when the C terminus of the third predicted ORF (170cg) was deleted by *Not*I (Figure 3). A subclone containing a 5.2-kbp *Kpn*I-*Hin*dIII fragment (from position 49735 bp to 55009 bp in contig 9a36) that contained the entire 170cg ORF was constructed (Xhk5-4). The introduction of Xhk5-4 into strain 8-88 fully complemented the aerial hyphae defect

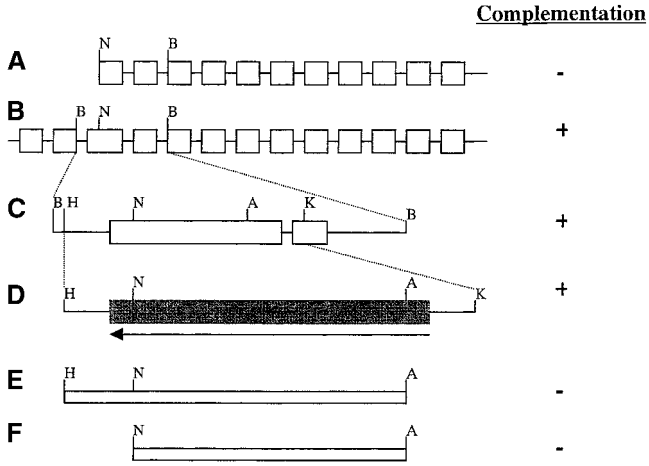

FIGURE 3.—Map of H57:G1 based on predicted ORFs (our analysis and http://www.mips.biochem.mpg.de/proj/neurospora/). Boxes indicate predicted ORFs (not drawn to scale). From left to right, the ORFs are 150cg to 270wg in contig 9a36 in MIPS Neurospora database (http://www.mips.biochem.mpg.de/proj/neurospora/). The direction of the predicted transcription of 170cg (*ham-2* ORF) is depicted in D by an arrow. The restriction sites in H57:G1 are indicated: N, *Not*I; B, *Bam*HI; H, *Hin*dIII; K, *Kpn*I; A, *Apa*I. + indicates that the introduction of a subclone of H57:G1 into 8-88 (Table 1) can restore normal aerial hyphae differentiation; − indicates that the construct does not complement the aerial hyphae defect. (A) *Not*I-3, (B) H57:G1, (C) *Bam*HI9-4, (D) Xhk5-4, (E) Xha4, and (F) AN3-2.

(Figure 3) and restored near normal growth rates of ~5–6 cm/day. However, the 8-88 (Xhk5-4) transformants still displayed the copious conidiation pattern of the *ahc* mutant.

To determine whether or not the introduction of Xhk5-4 restored heterokaryon formation capacity, Xhk5-4 was introduced into two different *ahc* strains that contained different auxotrophic markers and were also of different *het-c* specificity (8-88 and 8-16; Table 1). Vigorous heterokaryotic growth was observed in 2–3 days when conidial suspensions from 8-88 (Xhk5-4) and 8-16 (Xhk5-4) were co-inoculated onto a minimal medium. These data indicated that the ability to form heterokaryons via hyphal fusion was restored in *ahc* mutants by the introduction of Xhk5-4, but that vegetative incompatibility and a normal conidiation pattern were not. In a separate study, it has been determined that a different gene on H57:G1, termed *vib-1* for *v*egetative *i*ncompatibility *b*locked, encodes a mediator of *het-c* vegetative incompatibility and conidiation (Q. XIANG and N. L. GLASS, unpublished results).

The *ahc* mutation is a deletion: In other studies, it has been shown that escape from vegetative incompatibility is associated with deletion of *het* loci (DELANGE and GRIFFITHS 1975; SMITH *et al.* 1996). We therefore used restriction fragment length polymorphism analysis and Southern blots to determine whether the mutation in the *ahc* mutant is due to a deletion within the se-

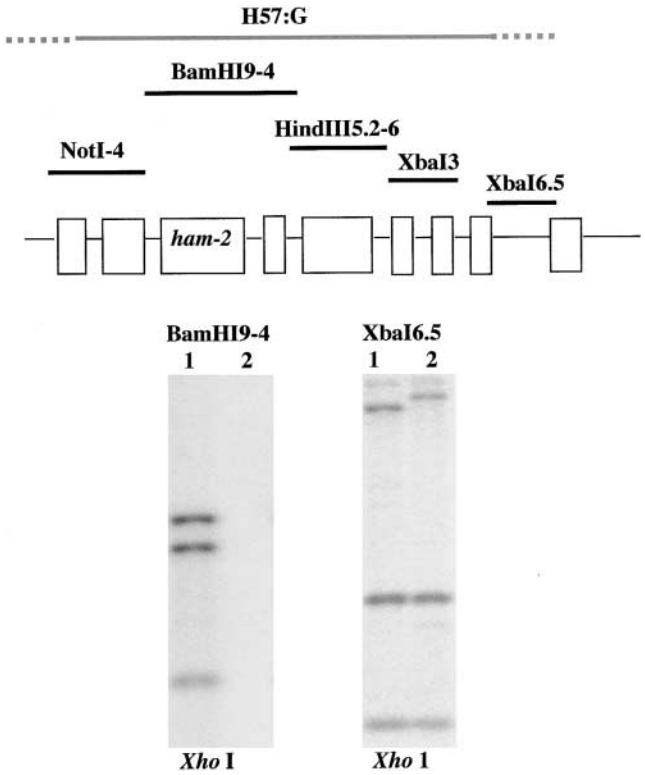

FIGURE 4.—Southern blot analysis showing that the *ahc* mutant contains a large deletion that includes the *ham-2* ORF. Restriction fragments in H57:G1 are depicted at the top of the figure with the predicted ORFs shown as boxes below (our analysis and from http://www.mips.biochem.mpg.de/proj/neurospora/). Probe used is shown at the top of the gel and enzyme used to digest genomic DNA at the bottom of the gel. Lanes 1: genomic DNA from wild-type strain C9-2 (Table 1). Lanes 2: genomic DNA from the *ahc* mutant (8-88). Sizes of the hybridizing fragments are, for the *Xba*I6.5 probe, 8116, 2500, and 794 bp and, for the *Bam*H19-4 probe, 3858, 3360, and 1885 bp. The *ham-2* ORF is within the *Bam*H19-4 fragment.

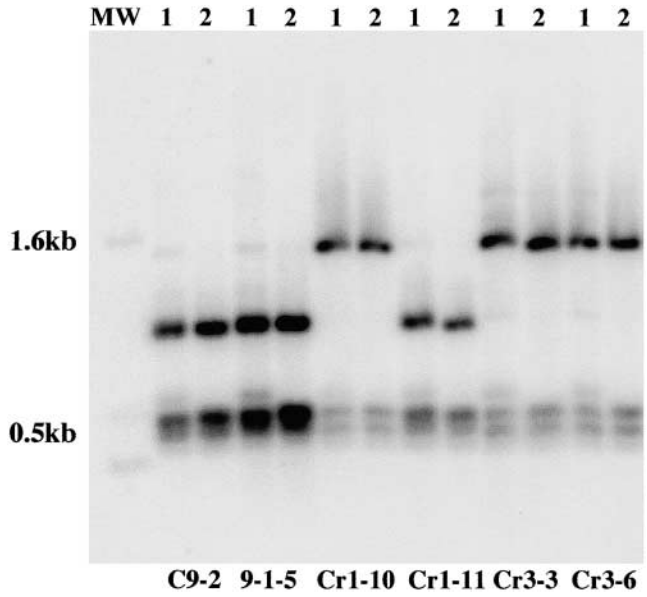

FIGURE 5.—Southern blot of genomic DNA from parental and *ham-2* RIP progeny. MW, molecular weight standards. Lanes 1: genomic DNA digested with *Sau*3A. Lanes 2: genomic DNA digested with *Dpn*I. C9-2 (Table 1): parental strain used for transformation with an internal fragment of *ham-2* (AN3-2; Figure 4). 9-1-5 (Table 1): strain crossed to C9-2 transformant. Cr1-10: progeny from the C9-2 (AN3-2) × 9-1-5 cross that contains restriction-site alterations in the *ham-2* resident sequence and displays the *ham-2* phenotype. Cr1-11: progeny that displays a *ham-2* phenotype, but without restriction site alterations at the *Sau*3A/*Dpn*I sites. Cr3-3 and Cr3-6: progeny from a Cr1-10 × R5-47 (Table 1) cross that displayed the *ham-2* phenotype and inherited the altered *ham-2* sequence from parent Cr1-10.

quences covered by the H57:G1 cosmid. Hybridization signals were detected in the 8-88 genomic blots probed by the *Xba*I6.5 fragment from cosmid H57:G1 (nucleotide position 67410–73921 in 9a36; Figure 4), but were absent when a 9-kbp *Bam*HI9-4 probe (49405–59272, containing the entire 170cg ORF) was hybridized to similar blots. These data indicated that the *ahc* mutant contains a deletion that includes 170cg plus other ORFs in this region.

Isolation of 170cg mutants: Because the *ahc* mutant contains a deletion of >9 kbp, we sought to isolate mutants that contained mutations only in the 170cg ORF. To isolate 170cg mutants, we chose to use RIP mutation (SELKER 1997). A 3-kbp *Apa*I-*Not*I internal fragment (AN3-2; Figure 3) of 170cg was cloned into pCB1004 and introduced into a C9-2. A C9-2 hygromycin-resistant transformant was crossed with a wild-type strain, 9-1-5 (Table 1). Approximately 10% (15/129) of the progeny from the cross showed shortened aerial hyphae, a slow growth rate, and orange bodies. We isolated hygromycin-sensitive progeny to select against the ectopic copy of 170cg and confirmed the absence of ectopic copies by Southern blot analysis (data not shown). We subsequently assessed these progeny for methylation and restriction-site differences within the resident 170cg sequence by Southern blot analysis (Figure 5). Genomic DNA from one of the progeny that displayed the mutant phenotype contained a restriction-site alteration at nucleotide position 975 in 170cg (Cr1-10 lanes) as compared to the parental controls (C9-2 and 9-1-5 lanes). In a cross of this strain (Cr1-10) with a wild-type strain (R5-47; Table 1), all of the progeny that showed the mutant phenotype inherited the altered sequence from Cr1-10 (Cr3-3 and Cr3-6 lanes). These results are consistent with the mutant phenotype of the progeny being caused by mutations induced by RIP within 170 cg. Because of the phenotypic similarities between a hyphal fusion mutant, *ham-1* (*h*yphal *a*nasto*m*osis; WILSON and DEMPSEY 1999; see below), and mutants with mutations in 170cg, we name this locus *ham-2*.

***ham-2* mutants showed aerial hyphae, hyphal fusion, and growth defects:** The *ham-2* mutant progeny displayed a slower growth rate (~3 cm/day), aerial hyphae defects, and occasional orange bodies (Figure 1). To

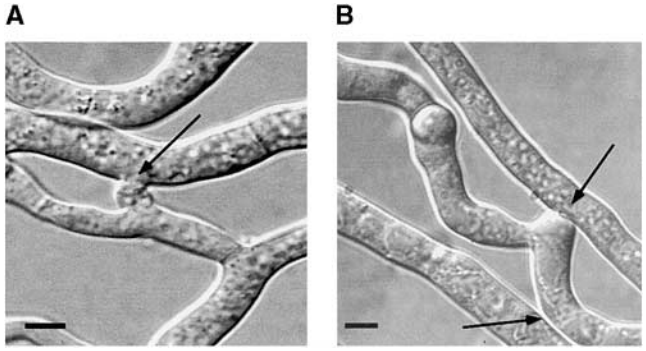

FIGURE 6.—Microscopic analysis of hyphal fusion bridges in the *ham-2* mutant as compared to wild type. (A) Wild-type strain C9-2 (Table 1). Note hyphal fusion bridge (arrow; bar, 10 μm). (B) Lack of hyphal fusion bridges in the *ham-2* mutant. Note similarity to wild type in hyphal architecture, but complete absence of hyphal fusion bridges (arrows; bar, 10 μm).

determine whether the *ham-2* mutants had a reduced capacity to form a heterokaryon, heterokaryon tests using conidial suspensions from *ham-2* mutants containing different auxotrophic markers (Cr3-6 + Cr3-20; Table 1) were performed. As with heterokaryons between *ahc* strains, heterokaryons between *ham-2* strains were not recovered after 5 days of incubation. Heterokaryon formation between *ham-2* mutants and wild-type strains was also delayed by 2 to 3 days. We determined the heterokaryon formation frequency of the *ham-2* mutant by plating different concentrations of *ham-2* conidia (Cr1-10) with a wild-type strain, FGSC 4564 (Table 2). The frequency of heterokaryon formation in the *ham-2* mutant was reduced 1000-fold over that of a wild-type strain and was similar to that of the *ahc* mutant.

The reduced frequency of heterokaryon formation between *ham-2* and wild-type strains and the difficulty in recovering *ham-2* heterokaryons is likely caused by a reduced capacity to undergo hyphal fusion. By contrast to wild-type colonies, hyphal fusion bridges were not observed in colonies of *ham-2* mutants (Figure 6), although the microscopic hyphal architecture of the *ham-2* mutant is similar to wild type, with wide trunk hyphae and smaller, meandering hyphae filling in the spaces between trunk hyphae. These hyphae are involved in hyphal fusion events in wild-type colonies (BULLER 1933).

***ham-2* mutants are affected in sexual reproduction:** Crosses between wild-type and *ahc* strains showed an ascus dominant defect that resulted in only 1% viable meiotic progeny (see above); homozygous *ahc* crosses were completely sterile. To determine whether *ham-2* mutants exhibit the same sexual defects as the *ahc* mutant, we crossed *ham-2* strains as both a male and a female in heterozygous and homozygous crosses (Figure 3, A, C, and D). When used as a female, a *ham-2* mutant (Cr3-12; Table 1) produced a few orange protoperithecial-like bodies and large orange bodies. Development of perithecia was not observed after fertilization with a wild-type strain (R1-08; Table 1) or with a different *ham-2* mutant (Cr3-17).

The inability of the *ham-2* mutants to make functional protoperithecia was complemented by heterokaryon formation between *ham-2* (Cr3-3) and FGSC 4564 (Table 1). In homozygous *ham-2* crosses, perithecial development was indistinguishable from wild-type crosses up to ~3–4 days postfertilization; however, further development of perithecia was blocked. When the internal contents of these perithecia were inspected, only a few minute asci were observed (Figure 2, C and D). Heterozygous crosses using *ham-2* mutants (Cr3-12) as a male (with R1-08; Table 1) were similar to wild-type crosses (Figure 2A). Perithecial, ascus, and ascospore development was similar to that of wild-type crosses, although full rosette development and ascospore ejection in these crosses was delayed by ~1 week. Thus, the ascus dominant defect of the *ahc* deletion mutant was not exhibited by *ham-2* RIP mutants.

***ham-2* encodes a novel putative transmembrane protein:** A single ORF is predicted in the 5.2-kbp Xhk5-4 fragment (http://www.mips.biochem.mpg.de/proj/neurospora/ and our analysis). The ORF begins at position 54407 bp (start codon) and stops at position 50837 bp (stop codon) in contig 9a36. The *ham-2* ORF has four introns and five exons and encodes a putative protein of 1087 amino acids (Xhk5-4; Figure 7). The protein has three putative transmembrane domains (http://bioweb.pasteur.fr/seqanal/interfaces/toppred.html) and is predicted to reside in the plasma membrane. BLAST searches (http://www.ncbi.nlm.nih.gov/blast/blast.cg) of the NCBI database with the predicted *ham-2* ORF revealed a number of hypothetical proteins of unknown function in a number of other eukaryotic organisms, especially within the predicted C-terminal region of HAM-2 (Figure 8). The C-terminal region of HAM-2 showed ~60% similarity (~40% identity) to the C-terminal region of hypothetical proteins in *Drosophila melanogaster*, *Caenorhabditis elegans*, *Schizosaccharomyces pombe*, *Saccharomyces cerevisiae*, and *Homo sapiens*. A region in the predicted amino terminal region of HAM-2 also shows similarity (although less than the C terminus) to the amino terminal region of these same hypothetical proteins in *D. melanogaster*, *S. pombe*, and *S. cerevisiae*.

DISCUSSION

In this study, we report the isolation and characterization of a gene required for hyphal fusion in filamentous fungi. Initially, we believed that the multiple defects displayed by the *ahc* mutant were due to mutations at a single locus. We subsequently showed that the aerial hyphae defects, female sterility, growth rate reduction, and hyphal fusion deficiency were due to the absence of a single gene, *ham-2*. The *ahc* mutant also showed suppression of vegetative incompatibility and conidiation defects. A second gene missing in the *ahc* deletion

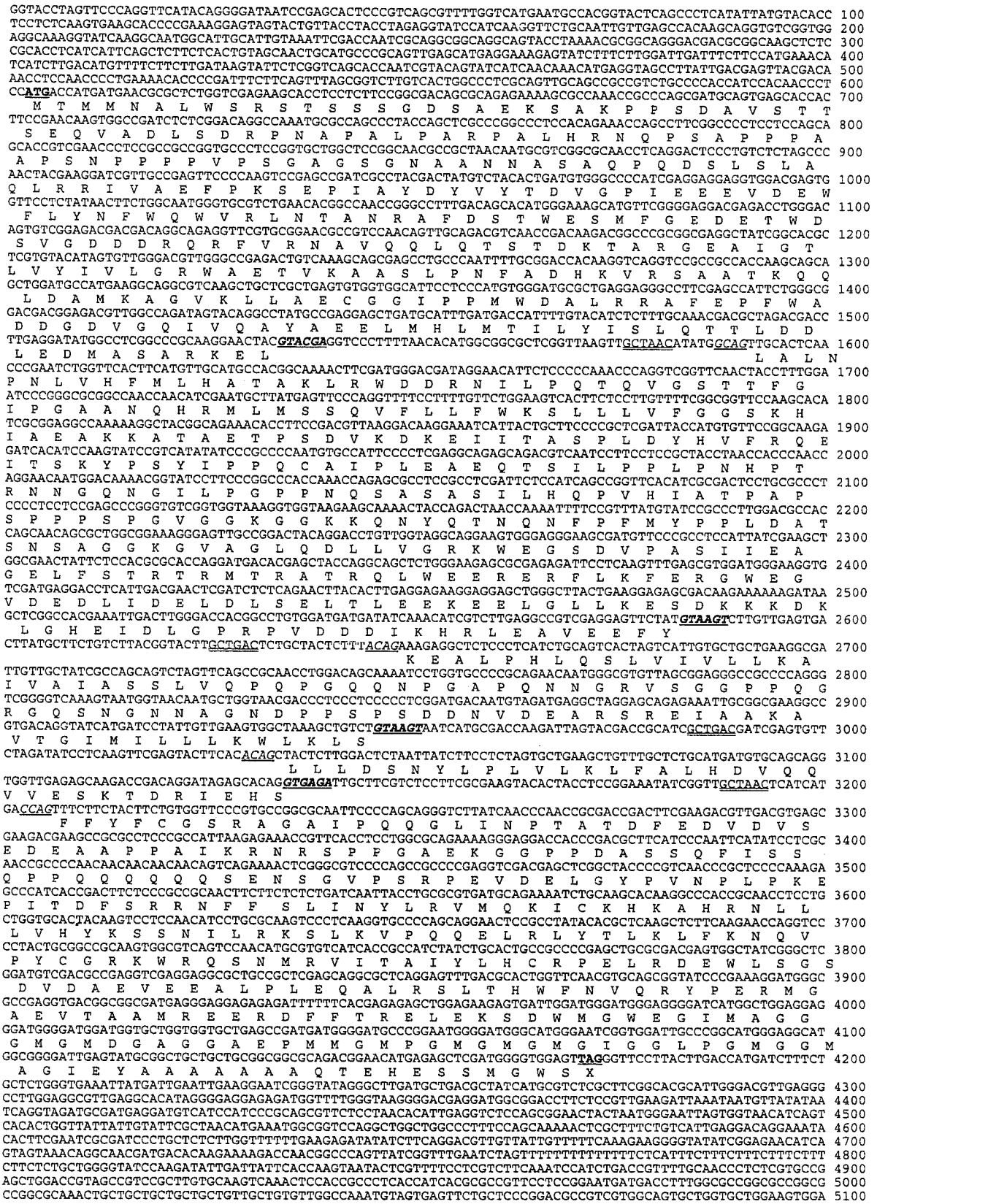

FIGURE 7.—Nucleotide sequences of the *ham-2* ORF obtained from the sequence of LGV from MIPS (http://www.mips.biochem.mpg.de/proj/neurospora/) and the Whitehead Neurospora genome project (http://www.genome.wi.mit.edu/annotation/fungi/neurospora/). The DNA sequence of the *ham-2* was identical in sequence from both sites. The predicted 1087-amino-acid (aa) ORF of *ham-2* was determined experimentally (this study) and computationally (our work and MIPS). The predicted translational start and stop sites are underlined and in boldface type. The predicted intron 5′ splice sites are in boldface and italic type and underlined, and the 3′ splice sites are underlined and italicized. The consensus lariat structure within the intron is double underlined. Obvious CAATT and TATA boxes were not observed in the promoter region of the *ham-2* gene.

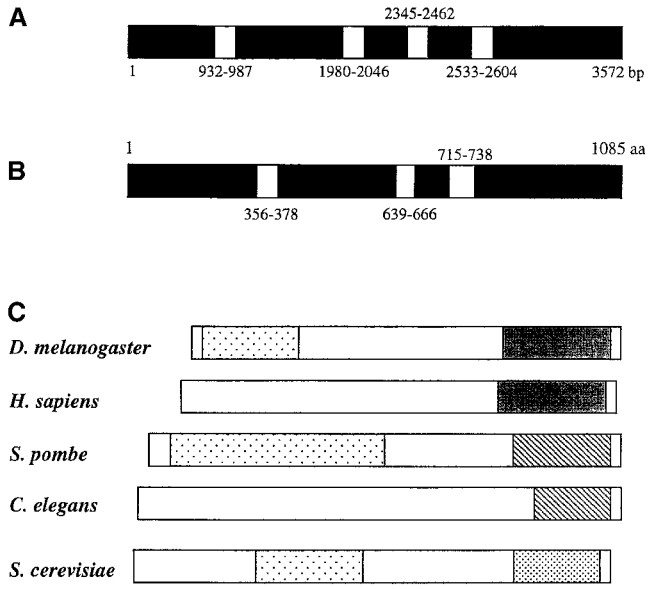

Figure 8.—(A.) The predicted nucleotide sequence of the open reading frame of HAM-2 based on our computational analysis and that of MIPS (http://www.mips.biochem.mpg.de/proj/neurospora/). The positions of four introns are indicated. (B) The predicted 1087-amino-acid sequence of HAM-2. The positions of the three putative transmembrane domains in HAM-2 protein based on computational analysis (http://bioweb.pasteur.fr/seqanal/interfaces/topred.html and http://130.237.130.31/tmap/single.html). (C) Regions in the hypothetical proteins in other organisms that show similarity to HAM-2. The putative gene products are CG11526 (AE003477) from *D. melanogaster*, hypothetical protein KIAA1170 (AB093 2996) from *H. sapiens*, hypothetical protein SPBC27B12.04c from *S. pombe*, hypothetical protein F10E7.8 from *C. elegans*, and predicted protein YN1127wp from *S. cerevisiae*. Identity and similarity, respectively, to a 150-aa C-terminal region of HAM-2 are 42 and 61% (Drosophila), 42 and 60% (human), 35 and 55% (*S. pombe*), 34 and 53% (*C. elegans*), 26 and 55% (*S. cerevisiae*). HAM-2 also has a less conserved region near the N terminus in Drosophila (23% identity/40% similarity over 250 aa), *S. pombe* (20% identity/38% similarity over 500 aa), and *S. cerevisiae* (27% identity/44% similarity over 200 aa) as indicated by the dotted boxes. BLAST searches were performed at the NCBI site (http://www.ncbi.nlm.nih.gov/BLAST/).

mutant, *vib-1*, encodes a protein required for mediating *het-c* vegetative incompatibility and proper conidiation pattern. The characterization of *vib-1* was aided by the isolation of mutants that do not include the *ham-2* locus and were therefore unaffected in hyphal fusion (Q. Xiang and N. L. Glass, unpublished results).

We named the locus required for hyphal fusion *ham-2* because of the similarity in phenotype of *ham-2* mutants to a previously described mutant in *N. crassa*, called *ham-1* (Wilson and Dempsey 1999). The *ham-1* mutant grows slightly more slowly than wild type (S. Haedo and N. L. Glass, unpublished results), is female sterile, has short aerial hyphae, and fails to undergo both self- and non-self-hyphal fusion. Hyphal fusion bridges have not been observed in *ham-1* or *ham-2* colonies. Although a few hyphal fusion mutants in filamentous fungi have been reported in the literature (Jacobson and Gordon 1988; Correll *et al.* 1989; Wilson and Dempsey 1999), this is the first report that we know of that describes the cloning and characterization of a locus required for hyphal fusion in filamentous fungi.

In addition to hyphal fusion, aerial hyphae formation, and growth rate defects, the *ham-2* mutant is also affected in sexual reproduction. Large orange bodies are occasionally formed in cultures of both the *ahc* and *ham-2* mutants. It is unclear what the origin of these bodies is, what conditions trigger their development, and whether their formation is related to growth and/or reproductive defects or other requirements. It is possible that the cause of the pleiotropic phenotype in the *ham-2* mutants may be the role that HAM-2 plays in different biological processes. In this hypothesis, *ham-2* mutants are not competent to undergo hyphal fusion because of a general biochemical defect. An example of such a scenario was shown by the isolation of a mutant in *S. cerevisiae* that fails to undergo mating cell fusion that has a defect in a glycerol transporter gene (*FPS1*) and thus accumulates high levels of intracellular glycerol (Philips and Herskowitz 1997). The mating cell fusion defect of the *fps1* mutant can be corrected by growth in 1 M sorbitol. Unlike the *fps1* mutant, the slow growth and hyphal fusion phenotype in the *ham-2* mutant cannot be corrected by growth on high osmotic medium (our unpublished observations) nor does HAM-2 show any sequence similarity to known transporters. Alternatively, the pleiotropic phenotype associated with *ham-2* mutants may result from the requirement for hyphal fusion events during various stages of growth and development in filamentous fungi. Hyphal fusion during vegetative growth is essential for formation of the hyphal network (Buller 1933) and for the formation of heterokaryons. Microscopically, we have not detected any hyphal fusion event in a *ham-2* colony. A possible role for hyphal fusion during vegetative growth is to facilitate the movement of materials from the established parts of a mycelium to the growing points. It is possible that, in a mutant with a severe hyphal fusion defect, the growth rate of the colony and aerial hyphae formation (which is also a tip growth process) may be affected.

The formation of female reproductive structures in ascomycete fungi may also require hyphal fusion processes, explaining why the *ham-2* mutant forms only a few protoperithecial-like structures. Hyphal fusion is believed to be required for the initiation of primordia in basidiomycetes (Kues 2000), the first step toward formation of a sexual reproductive structure. Hyphal fusion is also essential for entry into the sexual cycle in filamentous ascomycetes. During fertilization, reproductive hyphae, called trichogynes, protrude from protoperithecia, which are attracted to, and fuse with, male cells of the opposite mating type (conidia or hyphae;

Bistis 1981). The failure of the few protoperithecial-like structures observed in the *ham-2* mutant to develop following fertilization by conidia from the opposite mating type may be due to the failure of trichogyne-conidium fusion. If so, fusion competency is a requirement only for the female reproductive structures, as the *ham-2* mutant functions normally as a male.

Following fertilization, opposite mating-type nuclei proliferate in a common cytoplasm and eventually pair off and migrate into a hook-shaped structure, called a crozier (Raju 1980). Caryogamy occurs in the penultimate cell of the crozier, while hyphal fusion occurs between the terminal cell and the hyphal compartment subtending the penultimate cell. Homozygous crosses between *ham-2* mutants form only a few minute asci and no meiotic progeny. It is possible that sexual development is blocked in these strains at the time of crozier development due to a failure in a cell fusion event. We are currently investigating this hypothesis by more detailed cytological analysis in homozygous *ham-2* crosses.

The *ham-2* locus encodes a transmembrane protein. It is possible that HAM-2 encodes a receptor for hyphal fusion signals, a cortical tag for polarization of the cytoskeleton, or a protein involved in membrane fusion. Alternatively, HAM-2 could encode a plasma membrane protein that is involved in a process required for hyphae to become competent to undergo hyphal fusion. Heterokaryon formation between wild-type strains and *ham-2* was delayed, while *ham-2* heterokaryons were unrecoverable by traditional heterokaryon tests. We are currently assessing the hyphal fusion defects in the *ham-2* mutants during self- and non-self-hyphal fusion (between *ham-2* and wild-type strains) by examining hyphal fusion behavior by live cell microscopy and localizing HAM-2 in hyphae. These experiments will shed light on the role of HAM-2 during the hyphal fusion process.

Putative proteins with a high degree of similarity to HAM-2 have been identified in a wide range of eukaryotic organisms, although the function of these proteins in the biology of these organisms remains obscure. It is tempting to speculate that these proteins in other organisms may also be involved in cell fusion events. Interestingly, the *S. cerevisiae* gene (YN1127w; http://genome-www.stanford.edu/Saccharomyces/) that encodes the protein that shows similarity to HAM-2 is transcriptionally induced by exposure to pheromone, suggesting a possible role for this protein in mating cell fusion. Hyphal fusion in filamentous fungi may share features with both mating cell fusion in *S. cerevisiae* (Glass *et al.* 2000) and somatic cell fusion events resulting in syncytia, such as muscles, bones, and placenta formation in animals (Taylor 2000).

A feature that differentiates the *ahc* mutant from *ham-2* is the ascus dominant phenotype of *ahc* × wild-type crosses, as compared to *ham-2* × wild-type crosses. The *ahc* mutant contains a large deletion, while the *ham-2* mutants contain point mutations. The ascus dominant phenotype of *ahc* × wild-type crosses is reminiscent of *Asm-1* mutants (Aramayo and Metzenberg 1996). Pairing of *Asm-1* alleles in the diploid cell prior to meiosis is believed to be essential for productive ascospore formation, a phenomenon referred to as "meiotic transvection." In heterozygous *ahc* × wild-type crosses, genes within the deleted region in the *ahc* mutant lack a partner gene with which to pair and thus meiotic transvection may be invoked. By contrast, in heterozygous *ham-2* × wild-type crosses, the mutant and wild-type *ham-2* sequences are capable of pairing and thus do not display an ascus dominant phenotype. It will be of interest to determine whether a *ham-2* deletion mutant also displays an ascus dominant phenotype, similar to *Asm-1* deletion mutants.

The genetic and molecular dissection of the hyphal fusion process in *N. crassa* will reveal the role of this process in the various life stages of filamentous fungi as well as reveal common mechanisms in cell fusion events that are ubiquitous in biology. We believe that the formation of the hyphal network in filamentous fungi is necessary to integrate environmental signals, to undergo certain developmental processes, and for optimal growth rate. Hyphal fusion is therefore an essential feature of the filamentous fungal lifestyle.

We thank Dr. Dave Jacobson for help and advice on microscopy and Dr. Sergio Haedo for technical assistance with heterokaryon tests. This work was funded in part by a Natural Sciences and Engineering Research Council of Canada grant, a grant from Torrey Mesa Research Institute, Syngenta Research and Technology, and a National Institutes of Health grant (GM-60468-01) to N.L.G.

LITERATURE CITED

Akins, R. A., and A. M. Lambowitz, 1985 General method for cloning *Neurospora crassa* nuclear genes by complementation of mutants. Mol. Cell. Biol. **9:** 2272–2278.

Aramayo, R., and R. L. Metzenberg, 1996 Meiotic transvection in fungi. Cell **86:** 103–113.

Bistis, G. N., 1981 Chemotropic interactions between trichogynes and conidia of opposite mating-type in *Neurospora crassa.* Mycologia **73:** 959–975.

Buller, A. H. R., 1933 *Researches on Fungi.* Longman, London.

Carroll, A. M., J. A. Sweigard and B. Valent, 1994 Improved vectors for selecting resistance to hygromycin. Fungal Genet. Newsl. **41:** 22.

Correll, J. C., C. J. R. Klittich and J. F. Leslie, 1989 Heterokaryon self-incompatibility in *Gibberella fujikuroi* (*Fusarium moniliforme*). Mycol. Res. **93:** 21–27.

Davis, R. H., and F. J. De Serres, 1970 Genetic and microbial research techniques for *Neurospora crassa.* Methods Enzymol. **17A:** 79–143.

Delange, A. M., and A. J. Griffiths, 1975 Escape from mating-type incompatibility in bisexual (*A* + *a*) *Neurospora* heterokaryons. Can. J. Genet. Cytol. **17:** 441–449.

Glass, N. L., D. J. Jacobson and K. T. Shiu, 2000 The genetics of hyphal fusion and vegetative incompatibility in filamentous ascomycetes. Annu. Rev. Genet. **34:** 165–186.

Gooday, G. W., 1975 Chemotaxis and chemotrophism in fungi and algae, pp. 155–204 in *Primitive Sensory and Communication Systems: The Taxes and Tropisms of Microorganisms and Cells*, edited by M. J. Carlile. Academic Press, London.

Griffiths, A. J. F., and A. M. Delange, 1978 Mutations of the *a* mating-type gene in *Neurospora crassa.* Genetics **88:** 239–254.

Jacobson, D. J., and T. Gordon, 1988 Vegetative compatibility and

self-incompatibility within *Fusarium oxysporum* f. sp. *melonis*. Phytopathology **78:** 668–672.

Kues, U., 2000 Life history and developmental processes in the Basidiomycete *Coprinus cinereus*. Microbiol. Mol. Biol. Rev. **64:** 316–353.

Lee, S. B., and J. T. Taylor, 1990 Isolation of DNA from fungal mycelia and single spores, pp. 282–287 in *PCR Protocols: A Guide to Methods and Applications*, edited by M. A. Innis, D. H. Gelfand, J. J. Sninsky and T. J. White. Academic Press, New York.

McCabe, P. M., M. P. Gallagher and J. W. Deacon, 1999 Microscopic observations of perfect hyphal fusion in *Rhizoctonia solani*. Mycol. Res. **103:** 487–490.

Newmeyer, D., 1970 A suppressor of the heterokaryon-incompatibility associated with mating type in *Neurospora crassa*. Can. J. Genet. Cytol. **12:** 914–926.

Perkins, D. D., 1984 Advantage of using the inactive mating type a^{m1} strain as a helper component in heterokaryons. Neurospora Newsl. **31:** 41–42.

Philips, J., and I. Herskowitz, 1997 Osmotic balance regulates cell fusion during mating in *Saccharomyces cerevisiae*. J. Cell Biol. **138:** 961–974.

Raju, N. B., 1980 Meiosis and ascospore genesis in *Neurospora*. Eur. J. Cell Biol. **23:** 208–223.

Rayner, A. D. M., 1996 Interconnectedness and individualism in fungal mycelia, pp. 193–232 in *A Century of Mycology*, edited by B. C. Sutton. University of Cambridge Press, Cambridge, UK.

Riquelme, M., C. G. Reynaga-Pena, G. Gierz and S. Bartnicki-Garcia, 1998 What determines growth direction in fungal hyphae? Fungal Genet. Biol. **24:** 101–109.

Sambrook, J., E. F. Fritsch and T. Maniatis, 1989 *Molecular Cloning: A Laboratory Manual*. Cold Spring Harbor Laboratory Press, Cold Spring Harbor, NY.

Saupe, S. J., 2000 Molecular genetics of vegetative incompatibility in filamentous ascomycetes. Microbiol. Mol. Biol. Rev. **64:** 489–502.

Saupe, S. J., and N. L. Glass, 1997 Allelic specificity at the *het-c* heterokaryon incompatibility locus of *Neurospora crassa* is determined by a highly variable domain. Genetics **146:** 1299–1309.

Saupe, S. J., G. A. Kuldau, M. L. Smith and N. L. Glass, 1996 The product of the *het-C* heterokaryon incompatibility gene of *Neurospora crassa* has characteristics of a glycine-rich cell wall protein. Genetics **143:** 1589–1600.

Schweizer, M., M. E. Case, C. C. Dykstra, N. H. Giles and S. R. Kushner, 1981 Identification and characterization of recombinant plasmids carrying the complete *qa-2+* cluster from *Neurospora crassa* including the *qa-1+* regulatory gene. Proc. Natl. Acad. Sci. USA **78:** 5086–5090.

Selker, E. U., 1997 Epigenetic phenomena in filamentous fungi: Useful paradigms or repeat-induced confusion? Trends Genet. **13:** 296–301.

Shiu, P. K. T., and N. L. Glass, 1999 Molecular characterization of *tol*, a mediator of mating-type-associated vegetative incompatibility in *Neurospora crassa*. Genetics **151:** 545–555.

Smith, M. L., C. J. Yang, R. L. Metzenberg and N. L. Glass, 1996 Escape from *het-6* incompatibility in *Neurospora crassa* partial diploids involves preferential deletion within the ectopic segment. Genetics **144:** 523–531.

Staben, C., and C. Yanofsky, 1990 *Neurospora crassa a* mating-type region. Proc. Natl. Acad. Sci. USA **87:** 4917–4921.

Taylor, M. V., 2000 Muscle development: molecules of myoblast fusion. Curr. Biol. **10:** R646–R648.

Toyoshima, C., M. Nakasako, H. Nomura and H. Ogawa, 2000 Crystal structure of the calcium pump of sarcoplasmic reticulum at 2.6 A resolution. Nature **405:** 647–655.

Vellani, T. S., A. J. F. Griffiths and N. L. Glass, 1994 New mutations that suppress mating-type vegetative incompatibility in *Neurospora crassa*. Genome **37:** 249–255.

Vogel, H. J., 1964 Distribution of lysine pathways among fungi: evolutionary implications. Am. Nat. **98:** 435–446.

Westergaard, M., and H. K. Mitchell, 1947 Neurospora V. A synthetic medium favoring sexual reproduction. Am. J. Bot. **34:** 573–577.

Wilson, J. F., and J. A. Dempsey, 1999 A hyphal fusion mutant in *Neurospora crassa*. Fungal Genet. Newsl. **46:** 31.

Wu, J., and N. L. Glass, 2001 Identification of specificity determinants and the generation of alleles with novel specificity at the *het-c* heterokaryon incompatibility locus of *Neurospora crassa*. Mol. Cell. Biol. **21:** 1045–1057.

Xiang, X., and N. R. Morris, 1999 Hyphal tip growth and nuclear migration. Curr. Opin. Microbiol. **2:** 636–640.

Communicating editor: R. H. Davis